Strain-Induced Modifications of the Band Structure of $In_xGa_{1-x}P$–$In_{0.5}Al_{0.5}P$ Multiple Quantum Wells

Kathryn Interholzinger, Dinesh Patel, Carmen S. Menoni, *Member, IEEE,* Prabhuran Thiagarajan, Gary Y. Robinson, *Fellow, IEEE,* and Julie E. Fouquet, *Senior Member, IEEE*

***Abstract*— The effect of strain on the band structure of $In_xGa_{1-x}P$–$In_{0.5}Al_{0.5}P$ multiple quantum wells (MQW's) has been investigated from high-pressure and low-temperature photoluminescence measurements. The biaxial strain in the wells was varied between $+0.6\%$ compressive to -0.85% tensile strain by changing the well composition x from 0.57 to 0.37. Strain increases the valence band offsets in either tensile or compressively strained structures. Whereas relatively insensitive to tensile strain, the valence band offsets showed a strong dependence on the magnitude of the compressive strain. Good agreement is found between the measured valence band offsets and those predicted by the model solid theory, except for the largest compressively strained MQW's, for which the model calculations underestimate the measured valence band offset. Strain and the associated variations in composition also modified the separation among the well states associated with Γ_{1c}, L_{1c}, and X_{1c}. From these results, the bandgaps of each conduction band extrema were calculated in $In_xGa_{1-x}P$ for $0.37 < x < 0.57$ and compared with the predictions of the model solid theory.**

***Index Terms*— Heterojunctions, photoluminescent materials/devices, pressure measurements, quantum wells, semiconductor heterojunctions, strain.**

I. Introduction

THE MAIN goal in the development of visible InGaP–InGaAlP heterostructure lasers has been to reduce the operating wavelength below 630 nm, without a significant deterioration of their output characteristics [1]. Several approaches have been used to achieve short-wavelength operation, of which the incorporation of biaxial strain in the laser active medium has yielded encouraging results [2]. The benefits of strain, which are mainly associated with the modifications of the valence band structure, have resulted in a significant reduction of the threshold current of InGaP–InGaAlP lasers operating at 633 nm [3], [4]. Similar improvements are expected at shorter wavelengths. However, the design and optimization of these shorter wavelength devices is more critical as the expected benefits of the valence band modification with strain start to compete with the unwanted effects that arise from changes in the conduction band as the separation between the indirect and direct conduction band minima is reduced with strain [5]. Improved laser performance can be realized with a complete understanding of the band structure and band alignment modifications which occur with strain.

In this paper, we present the results of a systematic study on the effect of strain on the electronic band structure of gas-source molecular beam epitaxy (GSMBE) $In_xGa_{1-x}P$–$In_{0.5}Al_{0.5}P$ multiple quantum wells (MQW's) grown on [100] GaAs substrates. The [100] biaxial strain in the well was varied from $+0.6\%$ compressive to -0.85% tensile by changing the In composition x from 0.57 to 0.37. The barrier In composition was selected equal to 0.5 because it provides the largest Γ bandgap discontinuity with the well material and it enhances the effect of the indirect X extrema. We focus on the analysis of the changes in the valence band offsets with strain and also describe the modifications of the well electronic structure with strain, both of which are determined directly from the experiments. Based on these results, we calculate the electronic structure of $In_xGa_{1-x}P$ for $0.37 < x < 0.57$ by correcting for confinement and strain effects. The results of our experiments are compared with the predictions of the model solid theory [6].

The valence band offsets of the strained $In_xGa_{1-x}P$–$In_{0.5}Al_{0.5}P$ heterostructures were determined from high-pressure and low-temperature experiments using the method described by Wolford *et al.* [7]. The valence band offsets increased nonlinearly with compressive strain and remained almost unchanged with an increase of tensile strain. This dependence on strain follows the trend predicted by the model solid theory [6] for the tensile strain but is considerably larger than that predicted by the model for compressive strain. As a test of the accuracy of our heterojunction band offsets values, we calculated the MQW electronic states using the envelope function approach [8] and found that these calculations compared well with the results of photoluminescence excitation (PLE) measurements conducted on the $In_xGa_{1-x}P$–$In_{0.5}Al_{0.5}P$ MQW's.

The modifications of the electronic structure of $In_xGa_{1-x}P$–$In_{0.5}Al_{0.5}P$ MQW's with strain are well explained by the changes in the band structure of the bulk alloy with In composition x and the additional contributions of the

Manuscript received July 28, 1997; revised September 25, 1997. This work was supported by the National Science Foundation under Grant DMR 9321422 and Grant ECS-9502888, and by the AFOSR under Contract F49620-93-1-0021.

K. Interholzinger was with the Department of Electrical Engineering, Colorado State University, Fort Collins, CO 80523-1373 USA. She is now with Advanced Energy, Milpitas, CA 94035 USA.

D. Patel, C. S. Menoni, and G. Y. Robinson are with the Department of Electrical Engineering, Colorado State University, Fort Collins, CO 80523-1373 USA.

P. Thiagarajan was with the Department of Electrical Engineering, Colorado State University, Fort Collins, CO 80523-1373 USA. He is now with AE Spectracom, St. Paul, MN USA.

J. E. Fouquet is with Hewlett Packard Laboratories, Palo Alto, CA 94303-0867 USA.

Publisher Item Identifier S 0018-9197(98)00343-1.

hydrostatic and shear components of the strain [9]–[11]. Below $x = 0.48$, the Γ_{1c}–L_{1c} and Γ_{1c}–X_{1c} separation in $In_xGa_{1-x}P$ are reduced. As a result, we observed a reduction in the separation of the well states associated with each band extrema in tensile strained MQW's, to the extent that in highly tensile strained MQW's, the lowest confined well state showed an L-like behavior [12]. However, in the compressive strained MQW's ($x > 0.48$), the well X_{1c} states separate from those associated with Γ_{1c} and we do not see any evidence of L_{1c}, consistent with the measured increase in the Γ_{1c}–L_{1c} and Γ_{1c}–X_{1c} separation in the bulk [9]–[11].

The unique behavior of the Γ, L, and X-like states was evidenced in the high pressure and low temperature photoluminescence (PL) data from their pressure rate of change, dE/dp. The Γ_{1c}, L_{1c}, and X_{1c} states in the MQW's shifted with pressure at rates of about 100, 60, and -20 meV/GPa, respectively, characteristic of other III–V semiconductor materials [13]. Upon extrapolating the energy-pressure data of the PL transitions to atmospheric pressure, the electronic structure of the MQW's was obtained. Further corrections for confinement and strain effects allowed us to obtain the electronic structure of bulk $In_xGa_{1-x}P$ for In compositions $0.37 < x < 0.57$.

II. Experimental Details

The $In_xGa_{1-x}P$–$In_{0.5}Al_{0.5}P$ MQW's used in these studies were grown by GSMBE on a semi-insulating [100] GaAs substrate with nominally lattice-matched compositions for the barrier. The growth of the $In_xGa_{1-x}P$–$In_{0.5}Al_{0.5}P$ MQW's was carried out at 530 °C at 1.0 μm/h, conditions which produced a disordered random alloy in bulk InGaP samples as previously determined by PL, PLE, and transmission electron microscopy [14], [15]. Each sample contained a buffer layer of GaAs 0.5 μm thick, followed by an $In_{0.5}Al_{0.5}P$ buffer layer 0.035 μm thick, the MQW region, and an $In_{0.5}Al_{0.5}P$ cap layer 0.1 μm thick. All layers were unintentionally doped. The MQW's consisted of 50 periods of 50-Å wells and 150-Å barriers. The well indium composition x and the corresponding strain were selected to be 0.37 (-0.85%), 0.41 (-0.51%), 0.48 (0%), 0.5 (0.11%), 0.53 (0.32%), and 0.57 (0.60%), with negative strain corresponding to tensile and positive to compressive relative to the GaAs substrate. An additional unstrained MQW structure consisting of 50 periods of 30-Å wells and 150-Å barriers was also grown. Varying the electron confinement energy with well width and the composition was essential for altering the separation among the well states, and thus observed recombination from L_{1c} [12].

The PLE measurements were performed at 10 K, with the samples mounted in a He-flow cryostat. PLE spectra were obtained from the 50 Å unstrained, -0.85% tensile and 0.60% compressive strain MQW's. The PLE spectra of these samples showed the presence of several confined states above the ground state, indicating the high material quality of the MQW's. The high-pressure and low-temperature PL experiments were conducted using the setup described in [16]. The PL from the MQW's was excited using the 458-nm (2.7 eV) line of an Ar^+ laser with power levels of $\sim$5 mW which correspond to power densities of $\sim$100 W/cm^2 at the sample. Typical PL spectra corresponding to transitions originating from conduction band states associated with Γ_{1c}, L_{1c}, and X_{1c} are shown in [12], and had FWHM of $\sim$17, $\sim$20, and $\sim$25 meV, respectively. The Stoke's shift determined from the PL and PLE peak energy difference was 18 ± 6 meV for the unstrained and compressively strained MQW's, where the lowest conduction band confined state is Γ-like. For the highly tensile-strained MQW, the PL and PLE peak energy difference was 40 meV. This large difference arises because the PL and PLE transitions originate from states associated with L_{1c} and Γ_{1c}, respectively [12].

We next discuss the salient features of the energy-versus-pressure diagram of each MQW, starting first with the unstrained system as we refer all other band structure modifications with strain to this structure. We include for completeness the analysis of the results from the unstrained and tensile-strained MQW's that led us to the identification of the L band [12]. In Section III-B, we show how the valence band offsets are directly calculated from the energy-versus-pressure data and vary with strain. In Section III-C, we calculate the conduction band structure of bulk unstrained $In_xGa_{1-x}P$ for $0.37< x < 0.57$ from the atmospheric pressure values of the transition energy of well states associated with Γ_{1c}, L_{1c}, and X_{1c} by correcting for confinement and strain effects. In Section III-D, we use the model solid theory to calculate the valence band offsets of the $In_xGa_{1-x}P$–InAlP heterostructures and the conduction band structure of $In_xGa_{1-x}P$ with strain and compare with our experimental results.

III. Results and Discussion

A. Experimental Results

The energy-pressure diagram of unstrained $In_{0.48}Ga_{0.52}P$–$In_{0.5}Al_{0.5}P$ is shown in Fig. 1. The pressure behavior of both the 50- and 30-Å MQW's is very similar. Four PL transitions were observed, one with a positive pressure coefficient (dE/dp) and three with negative dE/dp. The labeling of these transitions is consistent with the analysis of [12]. The transitions with negative dE/dp, labeled E2, E3, and E4, were associated with recombination from X_{1c} and shifted with pressure at a rate $dE/dp \approx -20$ meV/GPa [10]. Since E3 and E4 were observed over the whole pressure range of the experiments, we assigned them to the indirect recombination of photoexcited carriers from X_{1c} in the well ($X_{1c} - 1$ hh) and in the barrier ($X^b_{1c} - \Gamma^b_{1v}$), respectively [12]. E2, however, is only observed at high pressures after the lowest confined well state (Γ_{1e}) becomes resonant with X^b_{1c}. The onset of E2 takes place at 1.4 GPa in the 50-Å sample and at a lower pressure of 0.8 GPa in the 30-Å sample, due to the increase in electron confinement.

The PL transition with a positive dE/dp, labeled E1 in the 50-Å MQW's, shifted at a rate $dE/dp = (92 \pm 3)$ meV/GPa, a value typical of a Γ-like behavior [10]. By contrast, dE/dp in the 30-Å MQW was measured to be (60 ± 5) meV/GPa. This lower dE/dp transition in the 30-Å MQW's originates from a conduction band state with an L-like behavior [12]. Recombination from L_{1c}, labeled L1, is observed in the 30-Å MQW's since Γ_{1e} is shifted above L_{1c} due to the increased electron confinement. Using the

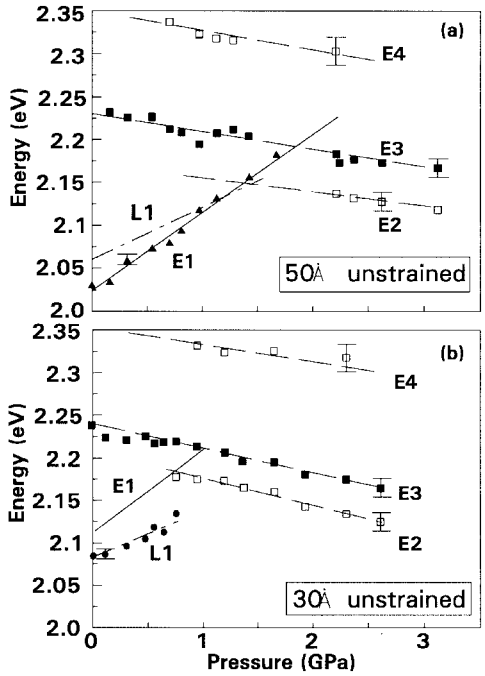

Fig. 1. Energy-versus-pressure diagram for the unstrained MQW's with (a) 50-Å and (b) 30-Å well width. A linear fit to the data yielded the pressure coefficient and the atmospheric pressure value of each PL transition. The pressure behavior of E1 in the 30-Å MQW and that of L1 in the 50-Å MQW where these transitions were not observed is shown by the solid line in (b) and the dash–dotted line in (a).

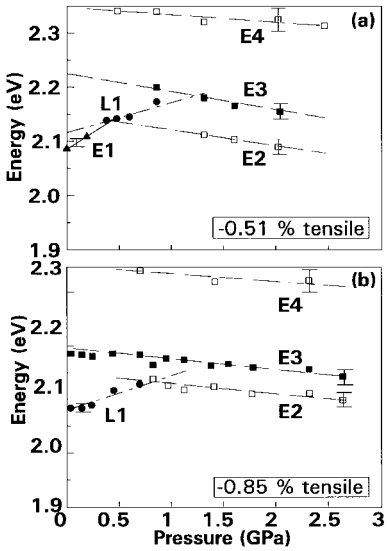

Fig. 2. Pressure dependence of the PL transitions in the (a) -0.51% and (b) -0.85% tensile strain MQW's.

atmospheric pressure values of L1 and E1 measured in the 30- and 50-Å MQW's, respectively, and accounting for the changes in carrier confinement with well width, we estimate that L_{1c} becomes the lowest conduction band state for well widths of less than 36 Å.

The energy-pressure diagrams of Fig. 1 also show an interesting behavior at a pressure close to the onset of E2, which reveals the importance of state mixing between the well Γ_{1e} and the barrier X_{1c}^{b} states. In the 50-Å MQW, E1 essentially disappears when E2 becomes the conduction band minima. In the 30-Å MQW, L1 also disappears at the onset of E2, although L1 is still at a lower energy than E2. This behavior is speculated to be the result of the competition between $\Gamma_{1c}-L_{1c}$ and $\Gamma_{1c}-X_{1c}^{b}$ transfer processes, the latter becoming dominant in the 30-Å MQW due to increased state mixing [17].

The energy-pressure data of the -0.51% and -0.85% tensile strain MQW's are shown in Fig. 2(a) and (b), respectively. The behavior of the PL transitions is similar to that measured in the unstrained MQW's. We identified the indirect E2, E3, and E4 transitions, which in these samples also shift at a rate $dE/dp \approx -20$ meV/GPa. We note, however, that with increased tensile strain, the E1–E3 separation was reduced as the Γ_{1c} bandgap increased with decreasing x below 0.48 and X_{1c} was split and lowered by the built-in [100] biaxial strain [5]. The E1–E2 separation was also decreased in the tensile structures compared to the 50-Å unstrained MQW's, reflecting the changes in the valence band offsets with strain.

The transition characterized by a positive dE/dp shifted at a rate of (60 ± 5) meV/GPa in the -0.85% strain MQW's, identical to that of L1 in the 30-Å unstrained MQW's. In the -0.51% strain MQW's it increased at a rate of $dE/dp = (110 \pm 5)$ meV/GPa to 0.5 GPa and at a slower rate $dE/dp \approx (60 \pm 5)$ meV/GPa at higher pressures, as shown by the solid and dash-dotted line of Fig. 2(a). The change in the slope is indicative of a pressure induced E1–L1 crossover occurring at 0.5 GPa.

As it will be shown in Section III-C, the atmospheric pressure values of L1 in the -0.51% and -0.85% tensile-strained MQW's are within 10% of those calculated from the L_{1c}-bandgap variation with composition of Bugaski *et al.* [11], and by adding the electron and hole confinement energies. It is important to mention, however, that in our experiments we could not discern if recombination occurs from L_{1c} or from an impurity state associated with L_{1c}, a situation that would lead to a larger uncertainty in the determination of the L_{1c} bandgap.

The pressure behavior of the different optical transitions observed in the $+0.32\%$ and $+0.60\%$ compressive strain structures is shown in Fig. 3. The equivalent diagram for the $+0.11\%$ strain MQW is omitted as it is very similar to that of the unstrained 50-Å MQW shown in Fig. 1(a). In the $+0.32\%$ and $+0.60\%$ compressively strained samples, the lowest energy transition identified as E1 shifted with pressure at a rate $dE/dp = (78 \pm 3)$ meV/GPa and (71 ± 3) meV/GPa, respectively, considerably lower than those determined in the unstrained and tensile strained MQW's. In the $+0.60\%$ sample, a weak PL transition (E5) at a higher energy than E1 and shifting at the same rate was also observed.[1] We argued before that a reduction of about 50% in dE/dp was indicative of an L-transition, however this is unlikely to be the case, as in the 50-Å compressively strained MQW's L_{1c} is predicted to be at a higher energy with respect to Γ_{1c} than in the 50-Å unstrained MQW's where the E1–L1 crossover is not observed. The origin of the dependence of dE/dp with strain

[1] E5 is a well transition possibly arising from recombination between the conduction band ground state and the split-off band.

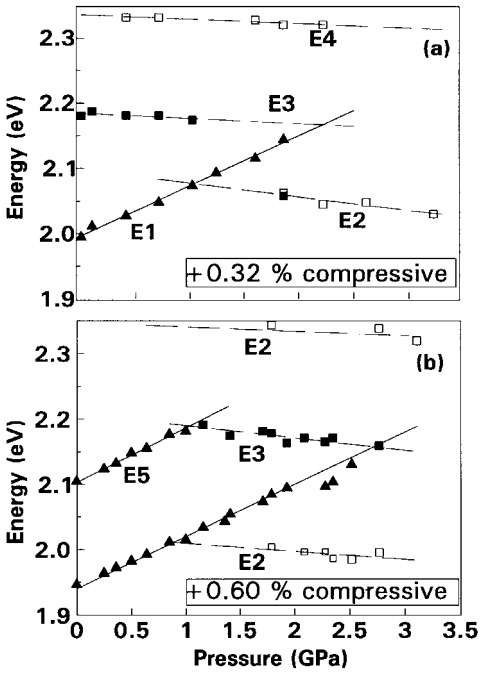

Fig. 3. Energy-versus-pressure diagram for the (a) +0.32% and (b) +0.60% compressive strain MQW's.

in the $In_xGa_{1-x}P$–$In_{0.5}Al_{0.5}P$ MQW's will be discussed in a separate publication.

The energy-pressure diagram of Fig. 3 also shows the X-like transitions E2, E3, and E4. With increased compressive strain the E1–E3 separation increased, as the Γ_{1c} bandgap of $In_xGa_{1-x}P$ is reduced in the In-rich alloys for $x > 0.48$. In spite of this bandgap reduction, the E1–E2 crossover was observed at a pressure of 1.2 GPa in the +0.32% strain MQW's and at 0.8 GPa in the +0.60% strain MQW's. The low pressure at which this crossover occurred indicates that most of the bandgap discontinuity has been accommodated in the valence band.

B. Determination of the Valence Band Offset

The valence band offset of the heterostructures was determined from the difference in the atmospheric pressure values of E4 and E2 and by adding the hole confinement energy E_h, $\Delta Ev = E4 - E2 + E_h$. E_h corresponds to the heavy hole confinement energy in the 50-Å unstrained and compressively strained MQW's, and to the light hole in the tensile-strained MQW's [18] and was calculated using the finite well approximation [8]. The electron and the heavy hole effective masses were obtained from a linear interpolation with alloy composition. The light hole effective mass was estimated from the analytical theory of People and Sputz, which is based on the Luthinger–Kohn 6 × 6 Hamiltonian [19]. The hole effective mass in the barrier material was taken to be equal to $0.22m_o$ [20]. ΔEv was calculated self-consistently by varying E_h until the E4–E2 energy difference equaled the measured value. The error in ΔEv was determined by taking into account the uncertainty in the E4 and E2 peak energies and that of the localization and excitonic energy associated with these transitions. ΔEv is a measure of the light hole valence band offset in the tensile-strained MQW's in which the light hole band is the top most confined state and of the heavy hole band offset in compressively strained MQW's in which the heavy hole is the valence band ground state.

The conduction band offset was calculated from E1 using the relationship $\Delta E_c = \Gamma_{1c}^b - E1 - \Delta Ev + e1 + E_L$, where Γ_{1c}^b is the direct bandgap energy of $In_{0.5}Al_{0.5}P$, e1 is the electron confinement energy, and E_L(∼18 meV) is a correction term to account for localization and excitonic effects [21]. Γ_{1c}^b was taken to be equal to 2.6 eV, as determined separately from low-temperature absorption measurements in a bulk epilayer grown as a reference in our laboratory. A similar value of the InAlP direct bandgap has been reported by Prins *et al.* [22], although it is 0.08 eV lower than that measured by Mowbray *et al.* [23]. The value of E1 in the −0.85% MQW where this transition was not observed was taken from the PLE experiments.

In Table I, we have compiled the measured ΔEv and ΔEc and the conduction to valence band offset ratios ($\Delta Ec/\Delta Ev$) for the strained and unstrained MQW's. Increasing tensile strain appears to increase ΔEv by an amount comparable to our measurement error which is only ±12%, and thus ΔEv is not very sensitive to the magnitude of the tensile strain used in our experiments. In compressively strained MQW's, ΔEv was found to vary more drastically with strain. ΔEc, on the other hand, decreases with either tensile or compressive strain. In spite of its decrease with strain, the electron potential discontinuity remains large in excess of 300 meV. Such a large conduction band discontinuity would be advantageous to reduce electron thermal leakage, identified as the limiting factor in obtaining short-wavelength operation in InGaP lasers [2]. However, in the $In_xGa_{1-x}P$–$In_{0.5}Al_{0.5}P$ heterostructures, the electron confinement is modified by the presence of the barrier X_{1c}^b states, which provide an additional leakage path [24]. The data of Figs. 2 and 3 show that in the 50-Å MQW's increased tensile or compressive strain reduces the E2–E1 separation considerably compared to the unstrained structure, reaching values as low as 30 meV for the −0.85% MQW's and 80 meV for the +0.60% MQW's.

Comparison of our values of $\Delta Ec/\Delta Ev$ with those determined in the $In_xGa_{1-x}P$–$In_{x'}(Ga_{1-y}Al_y)_{1-x}P$ system for similar In compositions x shows that $\Delta Ec/\Delta Ev$ is smaller for the MQW's with ternary barriers than in the case where quaternary barriers are used [25], [26]. This behavior indicates that $\Delta Ec/\Delta Ev$ varies with barrier composition in a fashion similar to that determined by Meney *et al.* [27] in unstrained and 1% strained $In_xGa_{1-x}P$–$In_{x'}(Ga_{1-y}Al_y)_{1-x'}P$ heterostructures.

C. Band Structure of Unstrained Bulk $In_xGa_{1-x}P$

The relevance of the results discussed above is that, besides providing a complete characterization of the band structure and band alignments of the $In_xGa_{1-x}P$—$In_{0.5}Al_{0.5}P$ MQW's, it allows us to infer the conduction band structure of bulk unstrained $In_xGa_{1-x}P$ as a function of composition. We can calculate the Γ_{1c}, L_{1c}, and X_{1c} bandgaps from the atmospheric pressure values of E1, L1, and E3 by correcting for confinement and strain effects. The electron and hole confinement energies were calculated with the envelope function

TABLE I
CONDUCTION AND VALENCE BAND OFFSETS AND OFFSET RATIO OF $In_xGa_{1-x}P$–$In_{0.5}Al_{0.5}P$ MQW'S

strain composition	-0.85% x=.37	-0.51% x=.41	0 x=.48	+0.11% x=.50	+0.32% x=.53	+0.60% x=.57
(ΔE_v ±.03) eV (exp)	0.27	0.25	0.2	0.21	0.26	0.36
(ΔE_c ±.03) eV (exp)	0.30	0.35	0.44	0.44	0.40	0.35
ΔE_c:ΔE_v	53:47	56:44	69:31	67:33	60:40	49:51

approach [8] using the measured band offsets and taking into account the variation of the electron and hole effective mass with strain. The hydrostatic and shear strain energy shifts of the valence and conduction band extrema were calculated using values of the hydrostatic and shear deformation potentials interpolated from the binary constituents taken from [6]. We ignored the electron confinement energy of L1 and E3 since they are small, due to the large effective mass of the L_{1c} and X_{1c} extrema, respectively.

We have plotted in Fig. 4 the Γ_{1c}–L_{1c} and Γ_{1c}–X_{1c} separation determined from our experiments and that predicted by Bugaski *et al.* [11]. Fig. 4 shows that L_{1c} becomes the conduction band minima around $x \sim 0.33$ and that for $x < 0.3X_{1c}$ is the conduction band minima. Increasing the In composition x above 0.48 increases the Γ_{1c}–X_{1c} separation. A similar behavior is expected for L_{1c}; however, the behavior was not identifiable from the experiments as the E1–L1 transition was preceded by E1–E2 which occurred at lower pressures for $x > 0.48$. Similar values for the Γ_{1c}–L_{1c} and Γ_{1c}–X_{1c} crossover compositions had been also determined from Hall measurements at high pressure [28] and piezomodulated reflectance measurements in bulk $In_xGa_{1-x}P$ alloys [9]. The agreement of our data and that of the band structure calculations of [10] is remarkable, considering that the determination of our bandgaps involves the use of parameters such as the hydrostatic and shear deformation potentials, which have not been directly measured for $In_xGa_{1-x}P$ and were interpolated from the binary constituents. However, we find that our measured Γ_{1c} bandgap is approximately 60 meV smaller than that predicted by Bugaski *et al.* [11] and also reported by Merle *et al.* [9]. Of the 60-meV difference between our Γ_{1c} values and those of Merle *et al.*, ~20 meV can be accounted for by the localization energy, and the rest is likely to arise from differences between the solution growth method employed by Merle *et al.* [9] and the GSMBE used in this work.

D. Comparisons to the Model Solid Theory

The bandgap energies and valence band offset energies for the $In_xGa_{1-x}P$–$In_{0.5}Al_{0.5}P$ heterostructure were calculated as a function of coherent strain in the $In_xGa_{1-x}P$ layer using the model solid theory of Van de Walle [7]. For the unstrained Γ_{1c} bandgaps at low temperature, the compositional dependence of $In_xGa_{1-x}P$ was taken to be $\Gamma_{1c}(x) = 1.41 + 0.73\,(1-x) + 0.7$

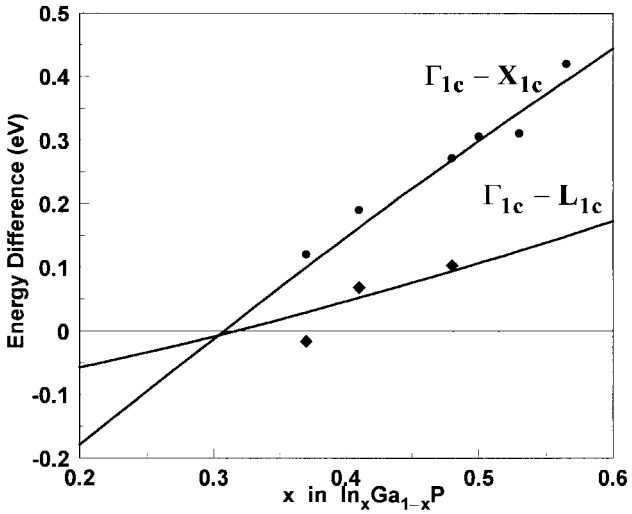

Fig. 4. Γ_{1c}–L_{1c} and Γ_{1c}–X_{1c} separation as a function of composition for unstrained $In_xGa_{1-x}P$. The Γ_{1c}–L_{1c} and Γ_{1c}–X_{1c} separations determined from the experiment are shown by the solid diamonds and circles, respectively. The solid lines are the predictions of the band structure calculations of [11].

$(1-x)^2$ [10], [11], and for $In_{0.5}Al_{0.5}P$, $\Gamma_{1c}^{b} = 2.60 \pm 0.03$ eV. The values of the elastic constants and deformation potentials for the binary compounds InP, GaP, and AlP were those given in [6]. For the absolute energy level $E_{v,ave}$ needed in the model solid theory, values of −8.04, −7.6, and −7.74 eV were used for InP, GaP, and AlP, respectively. These values correspond to the values given by Van de Walle [6] after a slight adjustment for GaP and AlP to bring the theoretical values of ΔEv into agreement with previously measured values for unstrained GaAs–InGaP [29] and InGaP–InAlP [16] heterojunctions. In InGaP, the spin-orbit split-off energy Δ_{so} is small and thus the coupling of the spin-orbit and light hole valence bands can be significant. The valence band coupling was taken into account by using a Luttinger–Kohn 6×6 Hamiltonian for a strained semiconductor [30]. The calculated transition energies from the conduction band to the heavy hole band $\Gamma_{1c} - \Gamma_{1vhh}$ and to the light hole band $\Gamma_{1c} - \Gamma_{1vlh}$ for InGaP alloys coherently strained to GaAs, along with the bandgap energy for unstrained bulk $In_xGa_{1-x}P$, are shown in Fig. 5(a). Also plotted in this figure are the dependence with strain of the singlet X_{1c}^{z} and doublet X_{1c}^{xy} bandgaps of the strained $In_xGa_{1-x}P$ alloys. Our experimental Γ_{1c} and X_{1c} bandgaps shown by the solid circles and diamonds,

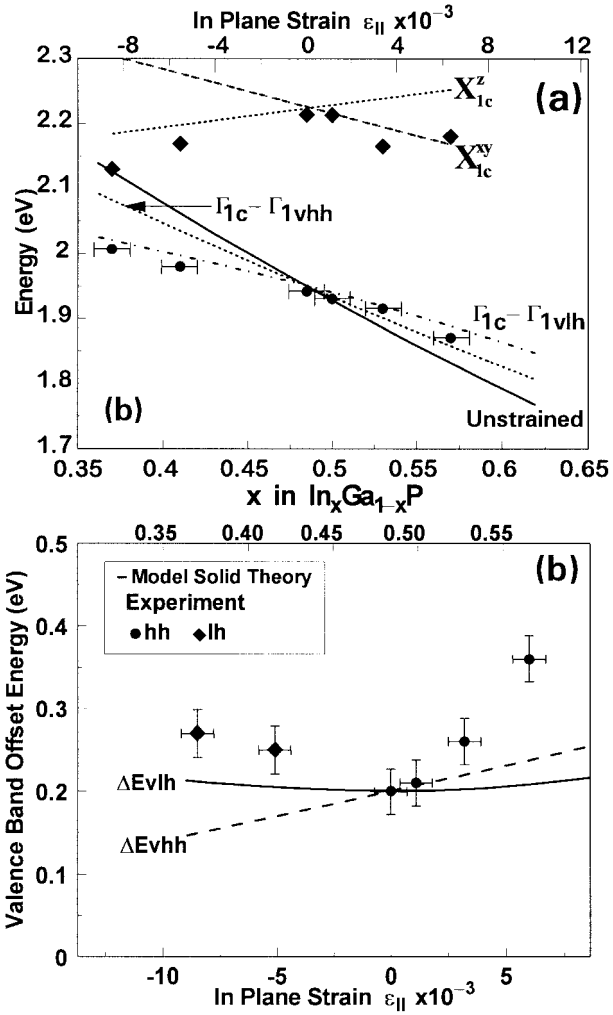

Fig. 5. Comparison of the measured (a) Γ_{1c} and X_{1c} bandgaps and (b) valence band offsets of strained $In_xGa_{1-x}P$, with the predictions of the model solid theory. In (a), the circles are the experimental Γ_{1c} bandgap obtained by subtracting the electron and hole confinement energy from the atmospheric pressure value of E1. The diamonds are the measured X_{1c} bandgap obtained from the atmospheric pressure value of E3 and by subtracting the hole confinement energy. The predictions of the model solid theory for the Γ_{1c}–Γ_{1vhh} and Γ_{1c}–Γ_{1vlh} bandgaps are shown by the dotted and dash–dotted lines, respectively. The X^z_{1c} and X^{xy}_{1c} bandgaps calculated from the unstrained value of X_{1c} using a deformation potential of 7 eV are represented by the dashed and dash–dotted lines, respectively.

respectively, closely follows the trend predicted by the model.

The valence band offset energies at the $In_xGa_{1-x}P$–$In_{0.5}Al_{0.5}P$ interface as a function of x calculated with the model solid theory are shown in Fig. 5(b). The increase of the heavy hole valence band offset ΔEvhh with x is due to a decrease of the Γ_{1c}-bandgap. The light hole valence band offset ΔEvlh, on the other hand, is almost constant with x because the spin-orbit coupling increases ΔEvlh in tensile strain. The experimental values of the valence band offsets have also been plotted in Fig. 5(b) for comparison. The general trend of the experimental results agrees with the model, however, we find that the model underestimates ΔEvhh for the highly compressively strained structures.

To estimate how significant the differences between the measured band offsets and those predicted by the model solid theory are, we calculated the confined energy levels in

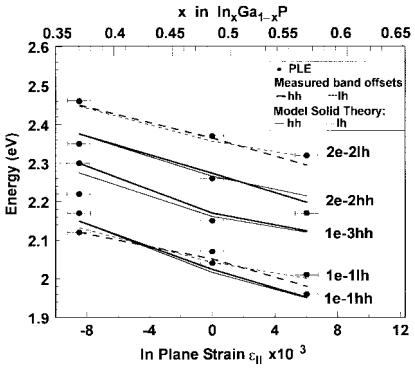

Fig. 6. Interband transition energies for -0.85, 0, and $+0.6$% strained $In_xGa_{1-x}P$–InAlP MQW's. The solid circles are the transition energies determined from PLE experiments. The heavy and light hole transition energies calculated with the values of the band offsets from this paper are represented by the thick solid and dotted lines, respectively, and those predicted by the model solid theory are represented by the thin solid and dotted lines, respectively.

the biaxially strained $In_xGa_{1-x}P$–$In_{0.5}Al_{0.5}P$ MQW's [8] and compared them with the results of the PLE measurements. This is shown in Fig. 6. Focusing on the higher energy transitions that are more sensitive to changes in the band offsets, we find that for the tensile-strained MQW's both our measured and the predicted band offsets can be used to estimate the transitions. For the $+0.60$% compressively strained MQW's, where our band offsets are 50% larger than those predicted by the model solid theory, we find that transition energies calculated using our value of the heavy hole band offset provides a slightly better fit to the data. However, a more extensive comparison on the differences between our band offsets and those predicted by the model solid theory requires the fitting of PLE interband transition energies obtained in MQW's with fixed strain and variable well width.

IV. Conclusion

We have studied the changes in the band structure of $In_xGa_{1-x}P$–$In_{0.5}Al_{0.5}P$ MQW's with strain. Strain modified the valence band offsets, which were found to increase with either tensile or compressive strain with respect to the unstrained value. The valence band offsets were relatively insensitive to an increase of tensile strain, while they increased nonlinearly with compressive strain. The trend in the valence band offset with strain was predicted by the model solid theory. While in good agreement with our results for the tensile and moderately compressively strained heterostructures, the model underestimated the strain dependence of the valence band offset in the highest compressively strained structures. The band offset changes with strain are accompanied by changes in the relative position of the well conduction band states, such that in narrow unstrained and highly tensile-strained MQW's the well ground state is associated with L_{1c}. From the simultaneous identification of MQW states associated with Γ_{1c}, L_{1c}, and X_{1c}, the band structure of unstrained $In_xGa_{1-x}P$ with $0.37 < x < 0.57$ was determined by correcting for confinement and strain effects. In bulk unstrained $In_xGa_{1-x}P$, Γ_{1c} was identified as the conduction band minima up to an In composition $x \sim 0.33$, at which L_{1c} becomes the conduction

band minima. The Γ_{1c}–L_{1c} crossover was followed by that of L_{1c}–X_{1c} which occurred at $x \sim 0.3$.

REFERENCES

[1] D. P. Bour, R. S. Geels, D. W. Treat, T. L. Paoli, F. Ponce, R. L. Thornton, B. S. Krusor, R. D. Bringans, and D. F. Welch, "Strained $Ga_xIn_{1-x}P/(AlGa)_{0.5}In_{0.5}P$ hetererostructure and quantum-well laser diodes," *IEEE J. Quantum Electron.*, vol. 30, pp. 593–607, 1994.

[2] D. P. Bour, D. W. Treat, K. J. Beernink, B. S. Krusor, R. S. Geels, and D. F. Welch, "610-nm band AlGaInP single quantum well laser diode," *IEEE Photon. Technol. Lett.*, vol. 6, pp. 128–131, 1994.

[3] D. P. Bour, D. W. Treat, R. L. Thornton, T. L. Paoli, R. D. Bringans, B. S. Krusor, R. S. Geels, D. F. Welch, and T. Y. Wang, "Low threshold, 633 nm, single tensile-strained quantum well $Ga_{0.6}In_{0.4}P/(Al_xGa_{1-x})In_{0.5}P$ laser," *Appl. Phys. Lett.*, vol. 60, pp. 1927–1929, 1992.

[4] J. Hashimoto, T. Katsuyama, J. Shinkai, I. Yoshida, and H. Hayasi, "Effects of strained-layer structures on the threshold current density of AlGaInP/GaInP visible lasers," *Appl. Phys. Lett.*, vol. 58, pp. 879–880, 1991.

[5] F. H. Pollak, *Semiconductors and Semimetals*, T. P. Pearsall, Ed. New York: Academic, 1990, vol. 32.

[6] C. G. Van de Walle, "Band lineups and deformation potentials in the model-solid theory," *Phys. Rev. B*, vol. 39, pp. 1871–1882, 1989.

[7] D. J. Wolford, T. F. Kuech, J. A. Bradley, M. A. Gells, D. Ninno, and M. Jaros, "Pressure dependence of $GaAs/Al_xGa_{1-x}As$ quantum-well bound states: The determination of valence band offsets," *J. Vac. Sci. Technol. B*, vol. 4, pp. 1043–1050, 1986.

[8] C. Cohen-Tannaoudji, B. Diu, and F. Laloë, *Quantum Mechanics.* New York: Wiley Interscience, 1977.

[9] P. Merle, D. Auvergne, H. Mathieu, and J. Chevallier, "Conduction band structure of GaInP," *Phys. Rev. B*, vol. 15, pp. 2032–2047, 1976.

[10] G. B. Stringfellow, "The importance of lattice mismatch in the growth of $Ga_xIn_{1-x}P$," *J. Appl. Phys.*, vol. 43, pp. 3455–3460, 1972.

[11] M. Bugaski, A. M. Kontkiewicz, and H. Mariette, "Energy bands of ternary alloy semiconductors: coherent-potential-approximation calculations," *Phys. Rev. B*, vol. 28, pp. 7105–7114, 1983.

[12] D. Patel, K. Interholzinger, P. Thiagarajan, G. Y. Robinson, and C. S. Menoni, "L-band recombination in $In_xGa_{1-x}P/In_{0.5}Al_{0.5}P$ multiple quantum wells," *Phys. Rev. B*, vol. 53, pp. 12633–12636, 1996.

[13] W. Paul and D. M. Warschauer, in *Solids Under Pressure.* New York: McGraw-Hill, 1963, p. 226.

[14] K. Mahalingam, N. Otsuka, M. J. Hafich, and G. Y. Robinson, "Correlation of spontaneous ordering in InGaP alloys with surface reconstruction," *Bull. Amer. Phys. Soc.*, vol. 38, p. 737, 1993.

[15] M. J. Hafich, H. Y. Lee, G. Robinson, D. Li, and N. Otsuka, "Quantum-well structures of InAlP/InGaP grown by gas-source molecular-beam epitaxy," *J. Appl. Phys.*, vol. 69, pp. 752–736, 1991.

[16] D. Patel, M. J. Hafich, G. Y. Robinson, and C. S. Menoni, "Direct determination of the band discontinuities in $In_xGa_{1-x}P/In_yAl_{1-y}P$ multiple quantum wells," *Phys. Rev. B*, vol. 48, pp. 18031–18036, 1993.

[17] T. Ando and H. Akera, "Connections of envelope functions at semiconductor heterointerfaces. II. Mixings of Γ and X valleys in $GaAs/Al_xGa_{1-x}As$," *Phys. Rev. B*, vol. 40, pp. 11619–11633, 1989.

[18] M. Watanabe, H. Matsura, and N. Shimada, "Investigation of tensile-strained InGaAlP multiple quantum well active regions by photoluminescence measurements," *J. Appl. Phys.*, vol. 76, pp. 7942–7946, 1994.

[19] R. People and S. K. Sputz, "Band nonparabolicities in lattice-mismatch-strained bulk semiconductor layers," *Phys. Rev. B*, vol. 41, pp. 8431–8439, 1990.

[20] T. Hayakawa, K. Takahashi, M. Hosada, S. Yamamoto, and T. Hijikata, "GaInP/AlInP quantum well structures and double heterojunction lasers grown by molecular beam epitaxy," *Jap. J. Appl. Phys.*, vol. 27, pp. L1553–L1555, 1988.

[21] O. P. Kowalski, J. W. Cockburn, D. J. Mowbray, M. S. Skolnick, R. Teissier, and M. Hopkinson, "GaInP–AlGaInP band offsets determined from hydrostatic pressure measurements," *Appl. Phys. Lett.*, vol. 66, pp. 619–621, 1995.

[22] A. D. Prins, J. L. Sly, A. T. Meney, D. J. Dunstan, E. P. O'Reilly, A. R. Adams, and A. Valster, "High pressure determination of AlGaInP band structure," *J. Phys. Chem. Solids*, vol. 56, pp. 349–357, 1995.

[23] D. J. Mowbray, O. P. Kowalski, M. Hopkinson, M. S. Skolnick, and J. P. R. David, "Electronic band structure of AlGaInP grown by solid-source molecular-beam epitaxy," *Appl. Phys. Lett.*, vol. 65, pp. 213–215, 1994.

[24] C. S. Menoni, O. Buccafusca, M. C. Marconi, D. Patel, J. J. Rocca, G. Y. Robinson, and S. Goodnick, "Effect of indirect Γ–L and Γ–X transfer on the carrier dynamics of InGaP/InAlP multiple quantum wells," *Appl. Phys. Lett.*, vol. 70, pp. 102–104, 1997.

[25] M. D. Dawson, G. Duggan, and D. J. Arent, "Optical measurements of electronic bandstructure in tensile strain GaInP–AlGaInP quantum wells," *Phys. Rev. B*, vol. 51, pp. 17660–17666, 1995.

[26] M. D. Dawson and G. Duggan, "Band-offset determination for GaInP–AlGaInP structures with compressively strained quantum well active layers," *Appl. Phys. Lett.*, vol. 64, pp. 892–895, 1994.

[27] A. T. Meney, A. D. Prins, A. F. Phillips, J. L. Sly, E. P. O'Reilly, D. J. Dunstan, A. R. Adams, and A. Valster, "Determination of the band structure of disordered AlGaInP and its influence on visible-laser characteristics," *IEEE J. Select. Topics Quantum Electron.*, vol. 1, pp. 697–706, 1995.

[28] G. D. Pitt, M. K. R. Vyas, and A. W. Mabbitt, "The conduction band structure of the $In_{1-x}Ga_xP$ alloy system," *Solid State Commun.*, vol. 14, pp. 621–624, 1974.

[29] J. Chen, J. R. Sites, I. L. Spain, M. J. Hafich, and G. Y. Robinson, "Band offset of $GaAs/In_{0.48}Ga_{0.52}P$ measured under hydrostatic pressure," *Appl. Phys. Lett.*, vol. 58, pp. 744–746, 1991.

[30] S. L. Chuang, *Physics of Optoelectronic Devices.* New York: Wiley, 1995.

Kathryn Interholzinger received the B.S. and M.S. degrees in electrical engineering from Colorado State University, Fort Collins, in 1993 and 1995, respectively. Her thesis work focused on the study of the band structure and band alignments in strained and lattice matched InGaP–InAlP multiple quantum wells.

She is presently working for Advanced Energy, Milpitas, CA.

Dinesh Patel received the B.S. and Ph.D. degrees in physics from the University of Surrey, England. His doctoral dissertation focused on the study of the temperature sensitivity of long-wavelength semiconductor lasers.

He is currently a Research Associate in the Department of Electrical Engineering at Colorado State University, Fort Collins. His research interests are in the optical diagnostics of long-wavelength semiconductor lasers, and III–V and II–VI heterostructures. He played a central role in developing electrooptical measurements as a function of hydrostatic pressure that have allowed for the identification of the effect of band structure changes in the output characteristics of semiconductor lasers. He is the author and co-author of more than 40 technical publications and conference presentations.

Carmen S. Menoni (M'93) received the Ph.D. degree in physics from Colorado State University, Fort Collins, in 1987.

In 1991, she joined the Department of Electrical Engineering at Colorado State University where she is presently an Associate Professor. Her research interests are in the characterization of semiconductor lasers and related heterostructures materials. In her current research, she is investigating the effect of band structure changes on the output behavior of long-wavelength semiconductor lasers in an effort to identify the dominant loss mechanisms. Differential carrier lifetime and gain measurements have been developed for these studies and are performed on long-wavelength devices as a function of temperature and hydrostatic pressure. Her research also involves the steady-state and time-dependent optical characterization of carrier localization effects in wide bandgap II–VI heterostructures. In collaborative projects with Colorado industries, she and her group have recently developed an ultrasensitive pollution monitoring instrument and are fabricating diffractive microoptics. She has authored and co-authored more than 30 technical papers, two book chapters, and numerous conference presentations. In 1997, she was local arrangement co-chair for the 55th Device Research Conference.

Dr. Menoni is a member of the American Physical Society.

Prabhuran Thiagarajan received the Ph.D. degree in electrical engineering from Colorado State University, Fort Collins, in 1996.

His areas of interest are in epitaxy of III–V compounds, semiconductor lasers, optics, and high-speed characterization of materials and devices. He is currently a Member of the Technical Staff at AE Spectracom, St. Paul, MN.

Gary Y. Robinson (S'66–M'69–SM'93–F'96) received the B.E.S. degree at the University of Texas, Austin, in 1965, and the M.S. and Ph.D. degrees from the University of California, Berkeley, in 1967 and 1969, respectively.

From 1970 to 1984, he was an Assistant Professor, Associate Professor, and Professor of Electrical Engineering at the University of Minnesota, Minneapolis, where he conducted research on electrical and metallurgical characterization of metal-semiconductor contacts on Si and the III–V semiconductors. In 1984, he started a new research group at Colorado State University, Fort Collins, where he is currently a Professor of Electrical Engineering and involved in the growth of III–V heterostructures by gas-source molecular beam epitaxy. He has taught short courses in the United States and Europe and has served in organizing committees for numerous conferences on the III–V semiconductors.

Prof. Robinson is a member of the AVS.

Julie E. Fouquet (S'84–M'85–SM'91) was born in Palo Alto, CA. She received the bachelor's degree in physics, with Phi Beta Kappa honors, in 1980 from Harvard University, Cambridge, MA, and the M.S. and Ph.D. degrees in applied physics from Stanford University, Palo Alto, CA, in 1982 and 1986, respectively.

She has been with Hewlett-Packard (HP) Laboratories since 1985, and is currently a Principal Project Scientist in the Communications and Optics Research Laboratory. She has investigated radiative recombination in a wide range of materials and devices using several techniques including time-resolved photoluminescence, photoluminescence excitation spectroscopy, and highly spatially resolved luminescence. Applications included high-brightness light-emitting diodes (LED's) for display and high-volume LED's for data communications. She has also investigated new optical measurement concepts and instrumentation, inventing the very low coherence superluminescent edge-emitting LED which is a key component in a number of HP's lightwave instruments. She currently leads a project to build a new type of optical cross-connect switch. She has been awarded three patents and has authored or co-authored 60 technical papers and 35 magazine articles on lasers and electrooptics and related topics.